SENSING OF CLOUDINESS WITH AN ORBITAL LASER RANGEFINDER

G.P. Kokhanenko, G.G. Matvienko, V.S. Shamanaev, Yu.N. Grachev, and I.V. Znamenskii

Institute of Atmospheric Optics,
Siberian Branch of the Russian Academy of Sciences, Tomsk
Received April 16, 1994

The capabilities of orbital lidars to sense cloudiness are analysed by the example of interpretation of the signals obtained with geodetic laser rangefinders. A method is described of reconstructing the optical characteristics of cloudiness from the measured duration of signal returns at predetermined levels. The probabilities of occurrence of various magnitudes of extinction coefficient and lidar ratio obtained by us are compared with the published data. Results of analysis of cloud returns of the rangefinder confirm the capability of space–based lidars to yield reliable information and allow us to provide a basis for guiding their development.

New possibilities in studying the atmosphere and underlying surface associated with the use of spaceborne lidars have stimulated the intensive development of a number of projects of the spaceborne lidars in the last few years. Some of these projects are in the closing stages. In particular, Russian BALKAN–1 lidar[1] has been prepared for launching aboard the SPEKTR module of the MIR orbital station, while the ALISA Russian–French lidar is planned to be placed aboard the PRIRODA module of the same station.[2] The LITE lidar is prepared for the NASA experiment with the Shuttle spacecraft.[3,4] In spite of the extensive model studies,[5,6] the problems facing the first lidar measurements are mostly technological (testing) than observational in character. This is caused by the necessity of obtaining the real data in order to elaborate techniques for lidar observations and their validation. The particular difficulties can emerge in interpretation of lidar returns from clouds that have essential spatial inhomogeneity.

Some problems of spaceborne laser sounding of clouds can be solved now on the basis of an analysis of signal returns of geodetic laser rangefinders that, unlike the lidars, were used in space many times.[7] The orbital laser rangefinders are capable of detecting the pulses reflected by the Earth's surface from the orbit few hundred kilometers high and can record the signal returns when the laser beam falls on a cloud. These returns may be considered as a prototype of lidar returns. In this paper we discuss the results of analysis of cloud signal returns obtained by laser rangefinders placed on board of geodetic satellites in Russia during 1982–1983.

The laser rangefinders had the receiving–transmitting systems with the following specifications:

Radiation wavelength	532 nm
Pulse energy	0.15 J
Pulse duration	10 ns
Diameter of the receiving telescope	0.27 m
Beam divergence ω_s	30"
Field of view angle ω_d	60"
Pulse repetition frequency	0.2 Hz

Based on the problems being solved a recording system of the rangefinder applied the threshold principle (Fig. 1). Four counters of time intervals (CTI's) were used that were triggered at different threshold power levels $P_1 \ldots P_4$. The lower level corresponded to the light power $P_1 = 1.7 \cdot 10^{-8}$ W incident on the receiving aperture of the rangefinder, and the upper one - to $P_4 = 1.1 \cdot 10^{-7}$ W. Time was counted off from the instant of pulse emission. The first CTI was switched on at the instant t_1 when the magnitude of the received power $P(t)$ was at the level P_1 and switched off at the instant t_2 thereby determining the threshold duration $\tau_1 = t_2 - t_1$. The threshold durations $\tau_2 \ldots \tau_4$ were measured analogously. All four threshold durations $\tau_1 \ldots \tau_4$ were recorded when the signal peak power $P_{max} > P_4$, and only one duration τ_1 when $P_1 < P_{max} < P_2$. The distance to the reflecting object was determined from the time T_0 between the instant of pulse emission and recording of maximum threshold durations (i.e., half the interval τ_4 in the case shown in Fig. 1). The cloudiness presence and the type of the underlying surface were additionally monitored by space photography. It should be noted that the specific character of problems being solved at that time obviated the need for simultaneous subsatellite measurements, and now it makes the interpretation of signal returns from clouds difficult.

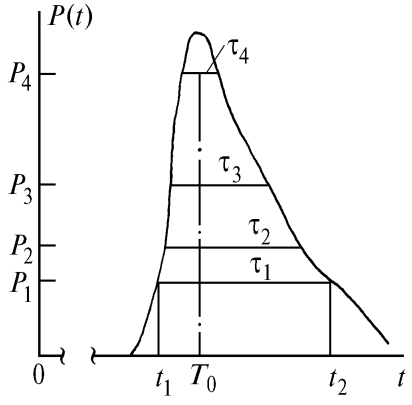

FIG. 1. Scheme for recording the signal return by the rangefinder with four threshold levels.

It should be emphasized that sufficiently high value of the threshold power P_1 was no bar to good reception of the signal returns from the underlying surface. However, at an

0235-6880/94/07 517-05 $02.00

orbit altitude of about 200 km, the signal returns from clouds with the extinction coefficient $\varepsilon < 10$ km^{-1} (the value most typical of upper air clouds) cannot be recorded by the rangefinder at all. This led to the fact that when laser beam fell on the clouds, the signal from them was recorded only in 5% of cases.

We have considered the measurement runs (several successive soundings with 5 s intervals between pulses) when we observed either the transition from underlying surface (sea, land) to cloudiness or conversely. In this case more reliable identification of cloudiness and determination of the upper boundary of cloudiness (UBC) are possible from the change of time of arrival of the next reflected pulse rather than from a photograph. Totally 56 acts of sounding the clouds with the UBC varying from 0.6 to 5 km were considered. The signal return was recorded only at the first threshold level in 28 cases, and all four levels were recorded only in 5 cases. The duration τ_1 at the first threshold level varied from 22 to 200 ns, which corresponded to the depth of sounding of the cloud $r_1 \approx c\tau_1/2$ ranging from 3 to 30 m.

A feature of the threshold principle of signal recording accepted in range finding in comparison with the amplitude–temporal principle typical of lidars calls for the development of special technique for signal conversion. A technique of modeling lidar return on the basis of a set of discrete threshold readings was applied. The foundation of the model was the signal calculated for horizontally homogeneous cloud in the single scattering approximation. Light power incident on a receiving aperture of the rangefinder is described by the laser sounding equation[8] (LSE)

$$P(r) = E_0 \frac{c\, S\, b(r)\, \varepsilon(r)}{2(R + r)^2} \exp\left(-2\int_0^r \varepsilon(r)\, dr\right), \qquad (1)$$

where E_0 is the energy of the sounding pulse, S is the receiver aperture, R is the distance from the cloud upper boundary, r is the current distance from the cloud upper boundary in the downward direction, ε is the extinction coefficient, b is the backscattering phase function, and c is the light speed. The atmospheric transparency is taken to be equal to 1 in Eq. (1), and the scattering coefficient of the cloud is taken to be equal to its extinction coefficient. The consequences of the fact that the multiple scattering is neglected in Eq. (1) will be considered below.

Let us simplify the LSE. Since the depth of penetration into the cloud r_1 is significantly less than R, the distance to the sounded volume in Eq. (1) is assumed constant $(R + r) \approx R_0 = cT_0/2$ and is determined by the time of arrival of the pulse T_0 (see Fig. 1). Let us also suppose that the backscattering phase function is constant within the cloud: $b(r) \equiv b$. Then LSE (1) assumes the form

$$P(r) = Ab\varepsilon(r) \exp\left(-2\int_0^r \varepsilon(r)\, dr\right), \; A = \frac{E_0 c\, S}{2R^2}. \qquad (2)$$

The standard techniques for solving the LSE that allow one to reconstruct the spatial distribution of $\varepsilon(r)$ for fixed $b(r)$ are inapplicable in our case since the amount of information is insufficient. We do not know the waveform of a signal and know only the threshold durations. For this reason we must use only simple models.

Depending on the number of threshold levels in the signal return, we used the models of cloud with the number of parameters changing from 1 to 3. The models differ in the form of the dependence $\varepsilon(r)$ at the upper boundary of a cloud and in the parameter b that either is included into a set of the parameters to be determined or is preset.

Model 1. Monotonic increase of ε is assumed in the form $\varepsilon(r) = ar^k$, where a and k are the parameters (this distribution of ε is characteristic of the upper boundary of stratus clouds[9]). The LSE has the form

$$P^{(1)}(r) = Abar^k \exp(-2ar^{k+1}/(k + 1)), \qquad (3)$$

containing three unknown parameters (b, a, and k). The signal returns that have no less than three threshold levels are processed by this model. The parameters are adjusted according to the scheme illustrated by Fig. 2. The real signal return is specified by the threshold durations τ_1, τ_2, and τ_3. The signal return $P(r) = P(ct/2 - R)$ is specified in the system of coordinates of Fig. 2 (the distance r from the model cloud boundary is plotted on the x axis) by the threshold durations $\rho_i = c\tau_i/2$. The model function $P^{(1)}(r)$ calculated for the given values of the parameters has the durations ρ'_1, ρ'_2, and ρ'_3 at the levels P_1, P_2, and P_3, respectively. We note that the start of the intervals $\rho_1 \ldots \rho_3$ of the signal return counted off from the cloud boundary ($r = 0$) is known with an error. The problem is to achieve the best correspondence of the calculated intervals ρ'_i with the measured ones ρ_i adjusting the parameters b, a, and k.

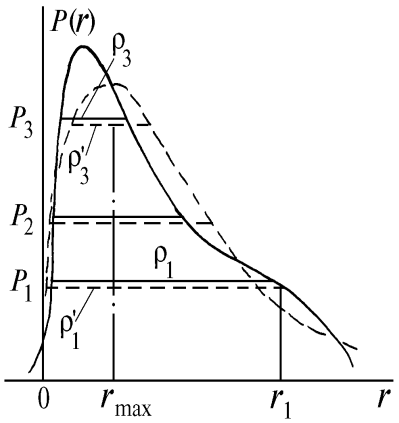

FIG. 2. Scheme for adjusting the model function for the signal return. Solid curve is the real signal return shape $P(r)$ with the measured threshold durations $\rho_1 \ldots \rho_3$. Dashed curve is the model function $P^{(1)}(r)$ calculated with threshold durations $\rho'_1 \ldots \rho'_3$. The condition $\rho'_3 = \rho_3$ is satisfied.

Recall that the model function $P^{(1)}(r)$ takes into account only the single scattering of radiation in a cloud. It is probable that the portion of multiple scattering is significant on the trailing edge of the pulse (at great depths of penetration of radiation into cloud). In this case it stronger affects the signal return durations at lower levels when the received power is low. So we always adjust $P^{(1)}(r)$ so that the calculated (ρ'_3) and measured (ρ_3) durations at the upper threshold level P_3 coincide. Setting a series of values b, we adjust the parameters a and k so that the discrepancy $N^{(1)}(b, a, k) = \sqrt{(\rho'_2 - \rho_2)^2 + (\rho'_1 - \rho_1)^2}$ is minimized under condition $\rho'_3 = \rho_3$. It should be noted that minimum

$N^{(1)}(b, a, k)$ may be nonzero and may significantly exceed the error in measuring the distance by the rangefinder (0.375 m). This is indicative of the unrealistic model. After adjusting the optimal parameters we may construct the model profile of the scattering coefficient $\varepsilon(r) = ar^{k}$. If the signal returns with four threshold levels were processed by model 1, the three upper levels P_2, P_3, and P_4 were used.

Model 2. The same dependence of $\varepsilon(r)$ as in the previous model was used but the value $b = 0.05$ was supposed to be known (as for Dermendjian $C1$ cloud model[10]). In this case two levels P_1 and P_2 are sufficient to estimate $\varepsilon(r)$. The discrepancy $N^{(2)}(a, k) = \sqrt{(\rho_1' - \rho_1)^2}$ was minimized adjusting the parameters a and k under condition $\rho_2' = \rho_2$. Two upper levels were used for processing the signals with three and four levels.

Model 3. The extinction coefficient ε is supposed constant with height. In this case Eq. (1) is simplified to the form

$$P^{(3)}(r) = Ab\,\varepsilon \exp(-2\,\varepsilon\, r) \qquad (4)$$

and we apply the technique analogous to the logarithmic derivative technique with durations at two threshold levels P_1 and P_2

$$\varepsilon = \frac{\ln P_2 - \ln P_1}{2(\rho_1 - \rho_2)},$$

and then determine the parameter b from Eq. (4).

Model 4. If we suppose $b = 0.05$ in model 3 (ε = const), we can calculate the dependence $\tau_i(\varepsilon)$ of the signal return duration at the upper threshold level P_i on the scattering coefficient ε and try to estimate the value of ε using only one threshold level. The dependence $\tau_i(\varepsilon)$ is nonmonotonic, and it turned out that almost half the signal returns had duration exceeding the maximum possible one for this model with the given value of the scattering phase function b. So the signal returns that had only one level P_1 were processed by the following way.

Let us suppose that the signal amplitude is known and is equal to the signal return power at the second threshold level P_2. In this case $\varepsilon = \ln(P_2/P_1)/2\rho_1$, and then the parameter b is found from Eq. (4). It is easy to see that this processing technique gives the upper estimate of ε and the lower estimate of b. We have also applied this technique for signal returns with two and three levels using the upper level for processing.

TABLE I. Results of signal returns processing by two models for dense clouds.

No.	ρ_1, m	ρ_2, m	ρ_3, m	Model 1					Model 2	
				$\varepsilon(r_{max})$, km^{-1}	b	k	$N^{(1)}$, m	T_{opt}	$\varepsilon(r_{max})$, km^{-1}	k
1	7.5	5.6	4.1	154	0.045	0.01	0.6	1.2	178	0.01
2	4.5	3.8	3.0	230	0.028	0.2	0.1	1.5	360	0.01
3	28.5	21.4	6.4	28	0.1	0.46	0.5	0.99	73	0.7
4	10.8	9.4	1.1	72	0.039	0.5	3.0	0.93	48	0.2
5	28.8	13.1	3.0	32	0.087	0.44	17.7	1.2	66	0.85

Table I shows as an example several signal returns that have three recorded threshold levels and the results of their processing by models 1 and 2. The value of the extinction coefficient $\varepsilon(r)$ is given for the point $r = r_{max}$ where the model functions $P^{(i)}(r)$ (i = 1, 2) reach their maxima (see Fig. 2). In addition to the reconstructed parameters ε, b, and k and the discrepancy $N^{(1)}$, Table I contains the optical depth $T_{opt} = \int_0^{r_1} \varepsilon(r)\mathrm{d}r$ (r_1 is the point at which the model function decreases down to the level P_1, see Fig. 2). The value $T_{opt} \approx 1$ is indicative of the possible noticeable contribution of multiple scattering at these depths of sounding.

Certainly, the degree of reliability of the information on optical parameters of clouds obtained by different models is different because the quantity of the employed experimental data is different as well as the conditions *a priori* supposed. It is manifested in the discrepancy in the estimates of the cloud parameters when we use different number of threshold levels of the same signal for reconstruction. An example (case 5 from Table I characterized by large discrepancy $N^{(1)}$) is shown in Fig. 3*a*. All proposed models were used for processing of this signal return that has three recorded threshold levels. The numbers adjacent to the curves indicate the serial numbers of models that were used for reconstruction of the signal return shape. The line segments intercepted with curve *1* at the threshold levels P_1, P_2, and P_3 represent the measured threshold durations. The profiles $\varepsilon(r)$ reconstructed by each model are shown in Fig. 3*b* (recall that model 4 gives the upper estimate of ε). The value of the scattering phase function b appeared to be equal to 0.09 for model 1 and 0.083 for model 3. The example is given of the case in which the significant deviation of the estimates of ε is observed for different models.

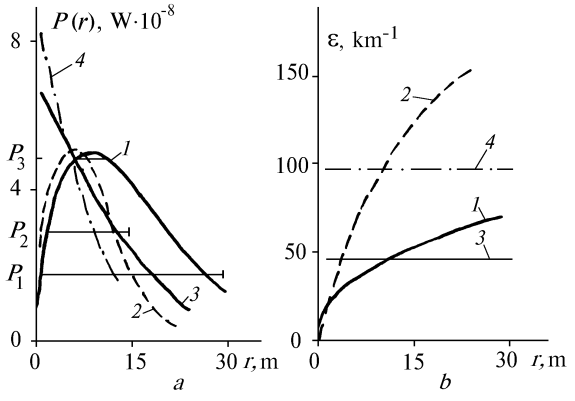

FIG. 3. An example of adjusting the model functions $P^{(i)}(r)$ (i is the serial number of the model applied, indicated by the numbers near the curves) for one of the real signal returns (a) and the reconstructed profiles $\varepsilon(r)$ at the upper cloud boundary for corresponding models (b).

Undoubtedly, model 1 has an advantage over the other models because it takes into account larger quantity of data (three measured durations) and there is no arbitrariness in setting b. Unfortunately, most experimental signal returns have only one or two levels. Application of different models for signal return processing (even for neighboring signal returns in the same measurement run) does not allow us to trace the variation of the cloud parameters from sounding to sounding. So we consider all optical parameters obtained by different processing techniques. In order to study the probability of occurrence of the given values of the extinction coefficient, the cases analogous to that shown in Fig. 3 were considered as four independent measurements of the optical parameters.

As the estimate shows, the reconstructed value of ε is within the limits from 14 to 500 km^{-1}. It is very large scatter of experimental data. (Recall that 95% of clouds that were obviously less dense were not recorded by the rangefinder.) The calculated accumulated probability $f(\varepsilon)$ of occurrence of clouds with different values of ε is shown in Fig. 4 (the values $\varepsilon(r_{max})$ are taken for models 1 and 2) in comparison with the data of Ref. 9 for clouds of different types. It is seen that in accordance with the published data, the probability of occurrence of very dense clouds also exists. Satisfactory agreement of our and independent results for dense Cu clouds confirms the reality of the obtained estimates of ε.

The results of estimates of the scattering phase function b somewhat stronger differ from that supposed in the models. Its average value b is equal to 0.07 for model 1 and 0.08 for model 3. At the same time, in 25% of cases (especially for model 3) b is greater than 0.1. This is essentially greater than physically justified values of b for droplet clouds.[10] As a rule, this is characteristic of the signal returns with long durations at the lower levels (100 ns and more). These signal returns poorly minimize the discrepancy when adjusting the parameters by the model with the preset value of b.

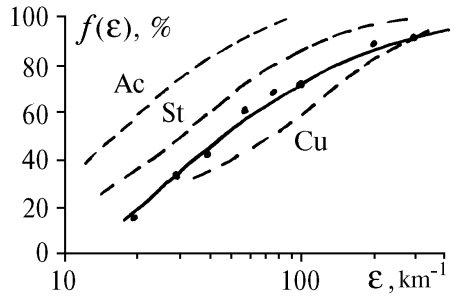

FIG. 4. Accumulated probability f(ε) of occurence of different values of the extinction coefficient ε from the results of processing of all sounding acts (solid curve). Dashed curves are for the experimental data for different cloud types taken from Ref. 9.

We suppose that such overestimated values can be explained by significant deviation of the characteristics of real clouds from our models. The following explanations are most probable. The first reason is possible presence of glint reflections in the signal return from oriented ice plates concentrated at the cloud top. The second reason is a step change in cloud altitude across a laser beam spot, comparable with its diameter. At least, and this is most essential, it is possible significant contribution of multiple scattering to signal return. Optical radius of laser beam spot at the cloud boundary $R_{opt} = \varepsilon R_0 \omega_d$ that primarily determines the portion of multiple scattering in the signal return, reaches $R_{opt} = 1$ for $\varepsilon = 30$ km^{-1}. It follows from the results of Ref. 5 that already at $R_{opt} = 1.5$ the signal return decrement decreases by a factor of 2.6 due to multiple scattering contribution progressively increasing with time. It leads to underestimated value of ε and overestimated value of b for our technique of data processing.

In conclusion it should be noted that the results obtained do not contradict with cloud physics. For this reason the data obtained with the use of laser rangefinders can be considered as the first experience on spaceborne laser sensing of the atmosphere. In addition, our estimates confirm the capabilities of spaceborne lidar to yield physically reliable data on cloud layers and provide a basis for guiding the development of spaceborne lidars. Undoubtedly, their application would call for further elaboration of mathematical methods of lidar signal return processing, which allow for real characteristics of broken clouds and contribution of multiple scattering. In addition, it might be expected that greater penetration depth and better accuracy of reconstruction of the optical parameters of cloudiness will be provide by the BALKAN and LITE lidars that have higher sensitivity and amplitude–temporal rather than threshold system of signal recording.

REFERENCES

1. Yu.S. Balin, V.V. Burkov, I.V. Znamenskii, et al., in: *Abstracts of Reports at the 15th Intern. Las. Rad. Conf.*, Tomsk (1990), Vol. **1**, pp. 12–14.
2. *International Special–Purpose Integrated Project PRIRODA. Scientific Program of Experiments* (Publishing House of the Institute of Radioelectronics, Russian Academy of Sciences, Moscow, 1991), 136 pp.
3. R.H. Couch, C.W. Rowland, K.S. Ellis, et al., Opt. Eng. **30**, No. 1, 88–95 (1991).
4. M.P. McCormic, D.M. Winter, E.V. Browell, et al., Bull. Amer. Meteorol. Soc. **74**, No. 2, 205–214 (1993).
5. G.M. Krekov, M.M. Krekova, and I.V. Samokhvalov, Issled. Zemli iz Kosmosa, No. 2, 44–51 (1988).
6. P.B. Russel, B.M. Morley, et al., Appl. Opt. **21**, 1541 (1982).
7. J.L. Bufton, Proc. IEEE **77**, No. 3, 71–88 (1989).
8. C.A. Northend, R.C. Honey, and W.E. Evans, Rev. Sci. Instr. **37**, No. 4, 393–400 (1966).
9. E.M. Feigelson, ed., *Radiation in the Cloudy Atmosphere* (Gidrometeoizdat, Leningrad, 1981), 280 pp.
10. D. Dermendjian, *Electromagnetic Scattering on Spherical Polydispersions* (American Elsevier, New York, 1969).